


Łukasz Ślusarczyk  orcid.org/0000-0002-3565-7868
slusarczyk@mech.pk.edu.pl

Emilia Franczyk

Institute of Production Engineering, Faculty of Mechanical Engineering, Cracow
University of Technology

THE EXPERIMENTAL DETERMINATION OF CUTTING FORCES IN A CUTTING ZONE DURING THE ORTHOGONAL TURNING OF A GRADE 2 TITANIUM ALLOY TUBE

EKSPERYMENTALNE WYZNACZANIE SIŁ W STREFIE SKRAWANIA PODCZAS TOCZENIA ORTOGONALNEGO RURY Z TYTANU GRADE 2

Abstract

This article presents the results of laboratory tests involving the measurement of cutting forces during the orthogonal turning of a tube made of GRADE 2 titanium alloy. The nominal diameter of the turned tube was $D = 60$ mm, and its wall thickness was 2.77 mm. For research purposes, a Kennametal chisel with an insert marked A3G0500M05P04DF and a holder marked A3SAR2520M0425-075-100 was used. An experimental research plan for variable cutting parameters (f, v_c) was developed according to the Taguchi method and statistical analysis of the results was performed using an ANOVA. Three series of tests were performed, one for each of the three different values of tube wall thickness ($a_p = 2.77, 1.77, 0.5$ mm). In accordance with the prepared test plan, nine trials were conducted within each series. Cutting forces were measured during each test with the use of a 3-axis Kistler 9257B piezoelectric dynamometer. DynoWare computer software was used for the archiving and analysis of measurement results.

Keywords: GRADE 2, cutting forces, ANOVA

Streszczenie

Artykuł prezentuje wyniki badań laboratoryjnych pomiaru sił skrawania podczas toczenia ortogonalnego rury z tytanu GRADE 2. Nominalna średnica toczonej rury wynosiła $D = 60$ mm, natomiast grubość ścianki 2,77 mm. Do badań wykorzystano przecinak firmy Kennametal o oznaczeniu płytki A3G0500M05P04DF, zamontowanej w oprawce A3SAR2520M0425-075-100. Eksperymentalny plan badań dla zmiennych parametrów skrawania (f, v_c) opracowano według metody Taguchi, natomiast statystyczne opracowanie wyników wykonano za pomocą analizy ANOVA. W czasie prac zostały przeprowadzone trzy serie prób trzech różnych wartości grubości ścianki rury ($a_p = 2,77; 1,77; 0,5$ mm). W ramach każdej serii zgodnie z opracowanym planem badań wykonano 9 prób. Pomiar sił skrawania był realizowany w każdej próbie za pomocą 3-osowego siłomierza piezoelektrycznego Kistler 9257B. Do archiwizacji i analizy wyników pomiarów zastosowano program komputerowy DynoWare.

Słowa kluczowe: GRADE 2, siły skrawania, ANOVA

1. Introduction

A properly conducted cutting process should guarantee high product quality and adequate tool durability [2–5]. Ensuring such a process requires the correct identification of the cutting zone status [1, 6]. The machining process is characterised by the following basic physical phenomena: large plastic deformations in the zone of concentrated tangential stresses; the movement of some of the workpiece material in the form of chips along the rake surface of the tool under conditions of varying mechanical and thermal stress; moving of some of the workpiece material along the flank surface of the tool, thus forming a machined surface [8, 9]. Proper analysis of the cutting zone performed in the design phase and during the selection of cutting tools is an important factor in order to select the best possible material configuration between the tool and the workpiece, and to determine the most appropriate tool stereometry [2, 3, 5, 8]. Experimental methods and methods based on theoretical models are used in the analysis of the machining zone [7]. Regardless of the choice of method, it is necessary to have knowledge about the phenomena that occur during the process of machining. Indicators coming from the cutting zone, such as the values of the cutting forces, the level of acoustic emission, thermal radiation and vibrations should be identified. On basis of these values, it is possible to control the cutting parameters [1, 9].

2. Conducted research

The laboratory stand was assembled with a set of measuring instruments used to record the components of the total cutting force. The arrangement of these instruments is presented in Fig. 1.

1. KISTLER 9257B 3 axis piezoelectric dynamometer,
2. KISTLER type 5070A multi-channel charge amplifier,
3. PC with a DynoWare software.

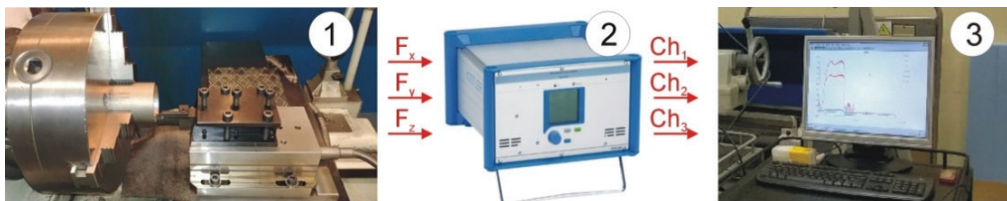


Fig. 1. The arrangement of measuring instruments used to record the components of the total cutting force

The cutting forces were recorded with a frequency of 1000 Hz. Such a measurement path enabled measurements of the components of the total cutting force with the following levels of inaccuracy: F_f (feed force) ± 0.25 N and F_c (tangential force) ± 1 N. Tool position in relation to the workpiece is presented in Fig. 2.

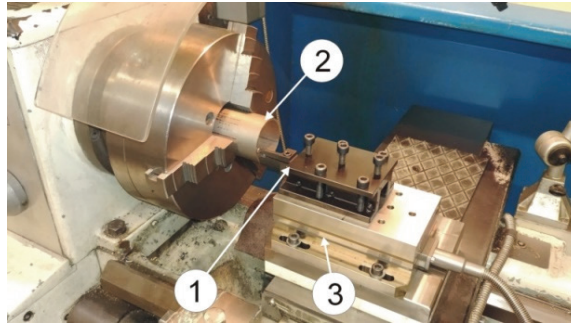


Fig. 2. Tool position in relation to the workpiece

where:

1. single-position tool holder with the insert installed,
2. a tube made of GRADE 2 titanium, diameter $D = 60$ mm,
3. a dynamometer mounted on the lathe slide.

A Kennametal chisel with an insert marked A3G0500M05P04DF and a holder marked A3SAR2520M0425-075-100 were used for the tests. The insert was made of KC5010 carbide with TiAlN coating. No coolant was used during the turning process. A photograph of the tool and 3D views of its face are shown below in Fig. 3. The presented 3D views were created by arranging successive 2D photos taken with the Keyence VHX-600 laboratory microscope. The face of the insert has a chip breaker and is characterised by a complex, symmetrical geometry.

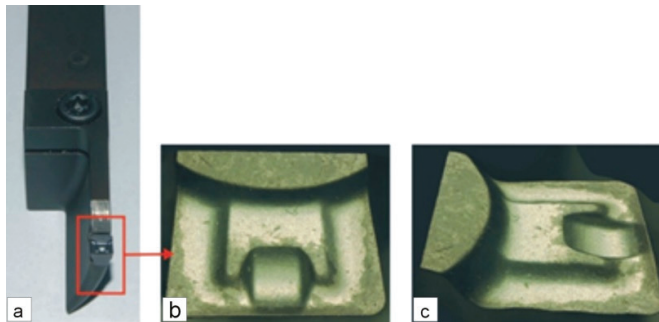


Fig. 3. a) The Kennametal tool, b) top and c) side views of the rake face

Geometrical dimensions of the A3G0500M05P04DF insert are shown in Table 1.

Table 1. Geometrical dimensions of A3G0500M05P04DF insert

| | |
|--|---------|
| | W [mm] |
| | RR [mm] |
| | T [mm] |
| | 5.00 |
| | 0.4 |
| | 4.5 |

On the basis of preliminary tests performed for the depth (width) of cutting $a_p = 2.77$ mm, a characteristic forms of the internal side of the chip associated with different velocities of its runoff on the tool face were observed (Fig. 4). Areas A and B were measured and determined on the chip and on the face of the insert. The widths of areas A on the rake face were 0.5 mm, while the width of area B was 1.77 mm.

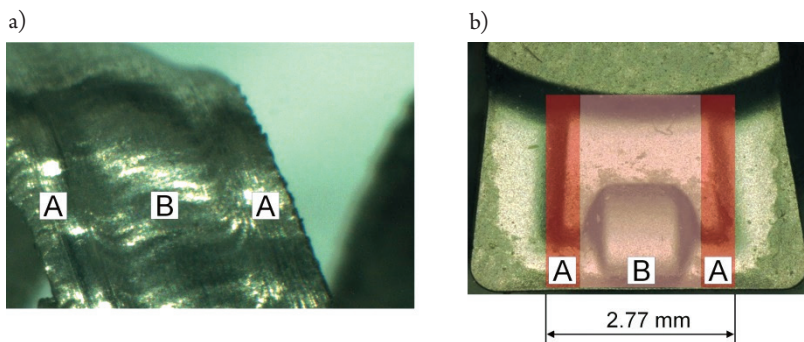


Fig. 4. a) Characteristic areas A and B on the chip surface and b) corresponding areas on the rake face of the insert

The workpiece was a tube made of GRADE 2 titanium alloy, diameter $D = 60$ mm. The chemical composition of the GRADE 2 titanium alloy, in accordance with the EN 10204-3.1 standard, is presented in Table 2.

Table 2. The percentage chemical composition of GRADE 2 titanium alloy

| | Fe | C | N | O | H | Ti |
|--------------|------|------|------|------|-------|------|
| GRADE 2 max. | 0.30 | 0.08 | 0.03 | 0.25 | 0.015 | Bal. |

Some properties of GRADE 2 titanium alloy are presented in Table 3.

Table 3. The properties of GRADE 2 titanium alloy

| | |
|------------------------|--|
| Melting Point | ca.1660 [°C] |
| Density | 4510 [kg*m ⁻³] |
| Modulus of Elasticity | 105 [GPa] |
| Specific Heat Capacity | 526 [J*kg ⁻¹ *K ⁻¹] |
| Thermal Conductivity | 16.4 [W*m ⁻¹ *K ⁻¹] |

3. Findings

Three series of tests were performed for three different values of pipe wall thickness ($a_p = 2,77; 1,77; 0,5$ mm). A research plan was generated using the Taguchi method. In accordance with the prepared test plan, nine trials were conducted within each series.

Parameters f and v_c were adopted as independent variables A and B, respectively. Ranges of variation of cutting parameters were determined on the basis of catalogue data. Table 4 presents assumed values of the cutting parameters.

Table 4. Values of cutting parameters

| Symbol | Cutting parameters | Parameter values | | |
|--------|--------------------|------------------|-------|-------|
| A | f [mm/rev] | 0.048 | 0.153 | 0.249 |
| B | v_c [m/min] | 60 | 100 | 140 |

The parameter values for the individual trials are given in the table below (Table 5).

Table 5. The parameter values for individual trials

| Test no. | A | B | f [mm/rev] | v_c [m/min] |
|----------|---|---|--------------|---------------|
| 1 | 1 | 1 | 0.048 | 140 |
| 2 | 1 | 2 | 0.048 | 100 |
| 3 | 1 | 3 | 0.048 | 60 |
| 4 | 2 | 1 | 0.153 | 140 |
| 5 | 2 | 2 | 0.153 | 100 |
| 6 | 2 | 3 | 0.153 | 60 |
| 7 | 3 | 1 | 0.249 | 140 |
| 8 | 3 | 2 | 0.249 | 100 |
| 9 | 3 | 3 | 0.249 | 60 |

At the stage of statistical analysis of the results, the S/N ratio was determined, the smaller-the-better criterion was adopted. According to Taguchi, this type of coefficient is used when it is appropriate to minimise some of the undesirable features of the product. The S/N ratio was calculated from the formula:

$$\frac{S}{N} = -10 \cdot \log \left(\frac{1}{2} \sum_{i=1}^n y_i^2 \right) \quad (1)$$

In accordance with the adopted test plan, the components of the total cutting force were measured. The influence of the variable cutting parameters (f and v_c) on the values of the total cutting force components (i.e., feed F_f and tangential F_t) was analysed. Tables 6, 9 and 12 present the obtained results of the S/N parameter and the average values of the individual components obtained in the individual tests system. Figures 5–10 graphically show the influence of specific cutting data on the values of the cutting force components.

Tables 7, 8, 10, 11, 13 and 14 present the statistical analysis of the test results (DF – degrees of freedom, Seq SS – sums of squares, Adj SS – adjusted sums of squares, and Adj MS – adjusted means squares).

Table 6. The obtained results of the S/N parameter and the average values of the individual components ($a_p = 2.77 \text{ mm}$)

| Test no. | v_c [m/min] | f [mm/rev] | $a_p = 2.77 \text{ mm}$ | | | |
|----------|---------------|--------------|-------------------------|----------------|-----------|----------------|
| | | | S/N F_f | F_f mean [N] | S/N F_c | F_c mean [N] |
| 1 | 140 | 0.048 | -45.0 | 177.8 | -47.5 | 236.2 |
| 2 | 100 | 0.048 | -45.6 | 190.1 | -46.5 | 179.2 |
| 3 | 60 | 0.048 | -44.2 | 161.3 | -47.4 | 234.0 |
| 4 | 140 | 0.153 | -47.4 | 234.4 | -55.2 | 573.8 |
| 5 | 100 | 0.153 | -47.8 | 245.3 | -55.3 | 578.5 |
| 6 | 60 | 0.153 | -47.9 | 248.7 | -55.3 | 578.3 |
| 7 | 140 | 0.249 | -48.4 | 261.1 | -58.3 | 825.4 |
| 8 | 100 | 0.249 | -49.5 | 296.7 | -58.5 | 840.2 |
| 9 | 60 | 0.249 | -49.7 | 303.0 | -58.5 | 842.3 |

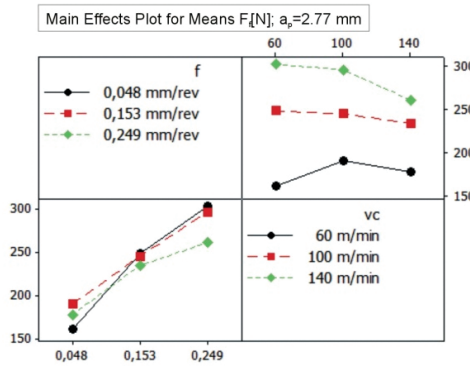


Fig. 5. The influence of the cutting data on the values of the cutting force components F_f , $a_p = 2.77 \text{ mm}$

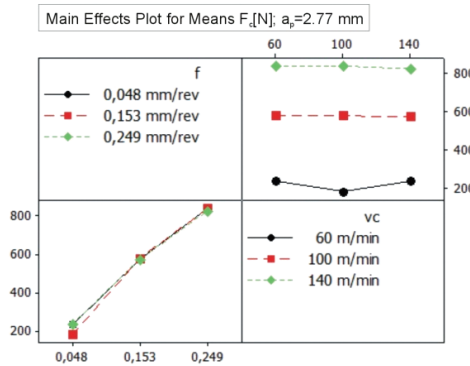


Fig. 6. The influence of the cutting data on the values of the cutting force components F_c , $a_p = 2.77 \text{ mm}$

Equations $F_f(f, v_c)$ and $F_c(f, v_c)$ for $a_p = 2.77$ mm are described below as Equations 2–3, respectively:

$$F_f(f, v_c) = 114.804 + 914.078 \cdot f + 0.379144 \cdot v_c - 3.63040 \cdot f \cdot v_c \quad (2)$$

$$F_c(f, v_c) = 70.2319 + 3206.02 \cdot f + 0.0975940 \cdot v_c - 1.18581 \cdot f \cdot v_c \quad (3)$$

Table 7. Analysis of variance for average value $F_p, a_p = 2.77$ mm

| Source | DF | Seq SS | Adj SS | Adj MS | F | p |
|----------------|----|---------|---------|---------|-------|-------|
| f | 1 | 55240.4 | 55240.4 | 55240.4 | 85.28 | 0.000 |
| v_c | 1 | 788 | 736.8 | 736.8 | 1.14 | 0.297 |
| $f \cdot v_c$ | 1 | 2557.6 | 2557.6 | 2557.6 | 3.95 | 0.059 |
| residual error | 23 | 14899 | 14899 | 647.8 | | |
| total | 26 | 73485.1 | | | | |

Table 8. Analysis of variance for average value $F_p, a_p = 2.77$ mm

| Source | DF | Seq SS | Adj SS | Adj MS | F | p |
|----------------|----|---------|---------|---------|--------|-------|
| f | 1 | 1734172 | 1734172 | 1734172 | 524.83 | 0.000 |
| v_c | 1 | 186 | 177 | 177 | 0.05 | 0.819 |
| $f \cdot v_c$ | 1 | 273 | 273 | 273 | 0.08 | 0.776 |
| residual error | 23 | 75998 | 75998 | 3304 | | |
| total | 26 | 1810629 | | | | |

Table 9. The obtained results of the S/N parameter and the average values of the individual components ($a_p = 1.77$ mm)

| Test no. | v_c [m/min] | f [mm/rev] | $a_p = 1.77$ mm | | | |
|----------|---------------|--------------|-----------------|----------------|-----------|----------------|
| | | | S/N F_f | F_f mean [N] | S/N F_c | F_c mean [N] |
| 1 | 140 | 0.048 | -41.8 | 122.0 | -44.3 | 162.8 |
| 2 | 100 | 0.048 | -42.2 | 128.8 | -44.6 | 169.1 |
| 3 | 60 | 0.048 | -42.9 | 138.8 | -44.9 | 175.9 |
| 4 | 140 | 0.153 | -43.6 | 150.3 | -51.8 | 386.1 |
| 5 | 100 | 0.153 | -44.3 | 163.4 | -51.4 | 369.2 |
| 6 | 60 | 0.153 | -45.4 | 184.6 | -52.2 | 404.3 |
| 7 | 140 | 0.249 | -44.7 | 170.9 | -55.0 | 560.0 |
| 8 | 100 | 0.249 | -45.7 | 190.5 | -55.0 | 561.0 |
| 9 | 60 | 0.249 | -46.6 | 212.8 | -55.3 | 579.5 |

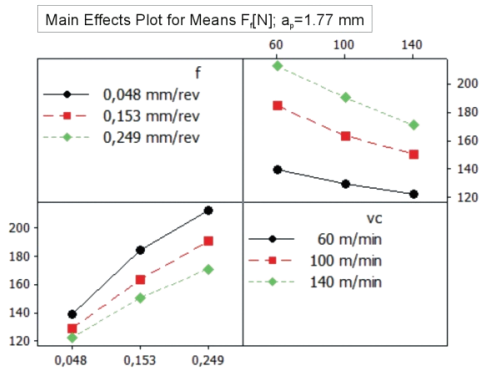


Fig. 7. The influence of the cutting data on the values of the cutting force components F_f , $a_p = 1.77$ mm

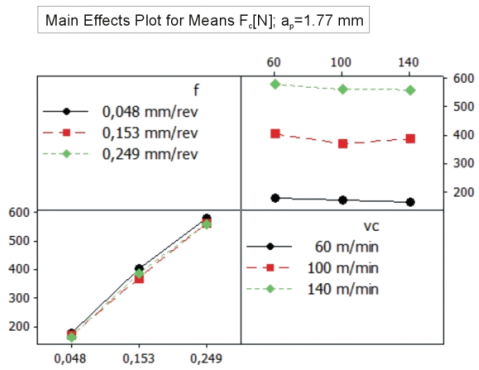


Fig. 8. The influence of the cutting data on the values of the cutting force components F_c , $a_p = 1.77$ mm

Equations $F_f(f, v_c)$ and $F_c(f, v_c)$ for $a_p = 1.77$ mm are described below as Equations 4–5, respectively:

$$F_f(f, v_c) = 131.599 + 464.212 \cdot f - 0.151348 \cdot v_c - 1.57527 \cdot f \cdot v_c \quad (4)$$

$$F_c(f, v_c) = 92.4486 + 2019.48 \cdot f - 0.151347 \cdot v_c - 0.401207 \cdot f \cdot v_c \quad (5)$$

Table 10. Analysis of variance for average value F_f , $a_p = 1.77$ mm

| Source | DF | Seq SS | Adj SS | Adj MS | F | p |
|----------------|----|---------|---------|---------|-------|-------|
| f | 1 | 17111.2 | 17111.2 | 17111.2 | 48.59 | 0.000 |
| v_c | 1 | 4327.6 | 4273.6 | 4273.6 | 12.14 | 0.002 |
| $f \cdot v_c$ | 1 | 481.5 | 481.5 | 481.5 | 1.37 | 0.254 |
| residual error | 23 | 8099.7 | 8099.7 | 352.2 | | |
| total | 26 | 30020 | | | | |

Table 11. Analysis of variance for average value F_c , $a_p = 1.77$ mm

| Source | DF | Seq SS | Adj SS | Adj MS | F | p |
|----------------|--------|--------|--------|--------|--------|-------|
| f | 1 | 712765 | 712765 | 712765 | 369.91 | 0.000 |
| v_c | 1 | 1289 | 1289 | 1289 | 0.66 | 0.423 |
| f^*v_c | 1 | 31 | 31 | 31 | 0.02 | 0.900 |
| residual error | 44318 | 44318 | 1927 | | | |
| total | 758402 | | | | | |

Table 12. The obtained results of the S/N parameter and the average values of the individual components ($a_p = 0.5$ mm)

| Test no. | v_c [m/min] | f [mm/rev] | $a_p = 0.5$ mm | | | |
|----------|---------------|--------------|----------------|----------------|-----------|----------------|
| | | | S/N F_f | F_f mean [N] | S/N F_c | F_c mean [N] |
| 1 | 140 | 0.048 | -32.6 | 42.1 | -37.2 | 71.6 |
| 2 | 100 | 0.048 | -32.4 | 41.3 | -34.4 | 51.5 |
| 3 | 60 | 0.048 | -32.5 | 41.3 | -35.0 | 55.5 |
| 4 | 140 | 0.153 | -36.3 | 64.0 | -42.1 | 124.9 |
| 5 | 100 | 0.153 | -38.9 | 86.1 | -43.6 | 147.5 |
| 6 | 60 | 0.153 | -39.7 | 90.8 | -43.9 | 153.7 |
| 7 | 140 | 0.249 | -39.1 | 87.1 | -45.9 | 194.0 |
| 8 | 100 | 0.249 | -40.7 | 105.7 | -44.7 | 167.1 |
| 9 | 60 | 0.249 | -42.8 | 135.7 | -49.2 | 284.3 |

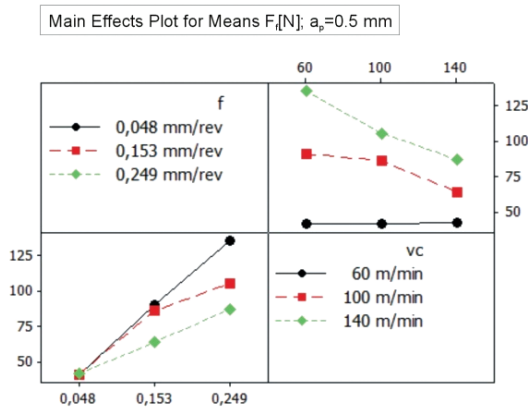


Fig. 9. The influence of the cutting data on the values of the cutting force components F_p , $a_p = 0.5$ mm

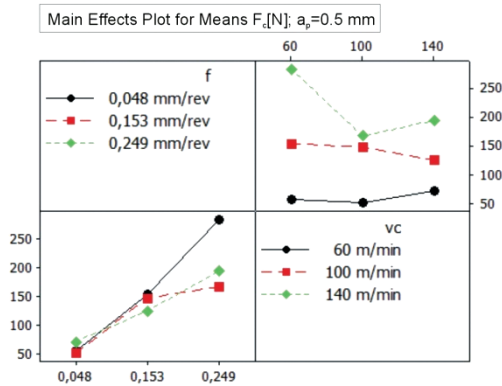


Fig. 10. The influence of the cutting data on the values of the cutting force components F_c , $a_p = 0.5$ mm

Equations $F_f(f, v_c)$ and $F_c(f, v_c)$ for $a_p = 0.5$ mm are described below as Equations 6–7, respectively:

$$F_f(f, v_c) = 11.2369 + 646.173 \cdot f - 0.151098 \cdot v_c - 3.07769 \cdot f \cdot v_c \quad (6)$$

$$F_c(f, v_c) = -33.3074 + 1434.19 \cdot f - 0.560723 \cdot v_c - 6.59926 \cdot f \cdot v_c \quad (7)$$

Table 13. Analysis of variance for average value F_p , $a_p = 0.5$ mm

| Source | DF | Seq SS | Adj SS | Adj MS | F | p |
|----------------|----|---------|---------|---------|-------|-------|
| f | 1 | 20833.7 | 20833.7 | 20833.7 | 44.06 | 0.000 |
| v_c | 1 | 2777.6 | 2694.7 | 2694.7 | 5.70 | 0.026 |
| $f \cdot v_c$ | 1 | 1838.1 | 1838.1 | 1838.1 | 3.89 | 0.061 |
| residual error | 23 | 10875.3 | 10875.3 | 472.8 | | |
| total | 26 | 36324.7 | | | | |

Table 14. Analysis of variance for average value F_c , $a_p = 0.5$ mm

| Source | DF | Seq SS | Adj SS | Adj MS | F | p |
|----------------|----|--------|--------|--------|-------|-------|
| f | 1 | 122816 | 122816 | 40939 | 27.53 | 0.000 |
| v_c | 1 | 109060 | 109060 | 109060 | 73.35 | 0.078 |
| $f \cdot v_c$ | 1 | 8451 | 8451 | 8451 | 5.68 | 0.026 |
| residual error | 23 | 34199 | 34199 | 1487 | | |
| total | 26 | 157015 | | | | |

4. Conclusions

During the preliminary laboratory tests, the orthogonal turning of a tube made of GRADE 2 titanium alloy was performed. The nominal tube diameter was $D = 60$ mm and its wall thickness was 2.77 mm. The length of the cutting edge of the insert was 5 mm. The insert had a symmetrical chip breaker on the rake face. By analysing the internal shape of the obtained chips, three work areas of the chip breaker were defined: two symmetrically distributed areas, marked in the article in Fig. 4 as A, with a width of 0.5 mm; and the area marked as B, with a width of 1.77 mm. As part of the basic research, three series of orthogonal turning tests were performed. In two series, where the wall thickness of the pipe was 2.77 and 1.77 mm the workpiece was in contact with the central part of the plate (area B), while for the wall thickness of 0.5 mm with the area marked as A. Each series consisted of nine runs in which the independent variables were f and v_c . Two components of the cutting force were obtained for each series – the feed component F_f and the main component F_c . On the basis of the ANOVA, dependencies and regression equations were determined for the mean values of the cutting force components in the functions of f and v_c . For three cutting depths, the F_f component decreased with the increase in v_c . The decreasing trend of the F_f component value is particularly visible for higher feed rates ($f = 0.249$ mm/rev and $f = 0.153$ mm/rev). An increase in v_c does not significantly change the F_c component. Higher values of the F_c component were obtained for larger feed values. The feed increase causes a linear increase in the F_f and F_c component values. Larger F_f values were observed for lower cutting speeds: $v_c = 60$ m/min and $v_c = 100$ m/min. The largest values of the cutting force components were obtained for the largest cutting depth $a_p = 2.77$, then 1.77 and 0.5 mm. The obtained dependencies will be used in further work to analyse the heat stream partition on the rake face of the insert.

References

- [1] Chomsamutr K., Jongprasithporn S., *Optimization Parameters of tool life Model Using the Taguchi Approach and Response Surface Methodology*, International Journal of Computer Science 9, 1/3, 2012, 120–125.
- [2] Ezugwu E.O., Bonney J., Yamane Y., *An overview of the machinability of aeroengine alloys*, Journal of Materials Processing Technology 134, 2003, 233–253.
- [3] Gawlik J., Zębala W., *Kształtowanie jakości wyrobów w obróbce precyzyjnej*, Mechanik, 2005, 12/2011.
- [4] Kramar D., Kopač J., *High performance manufacturing aspects of hard-to-machine materials*, Adv. Prod. Eng. Manag, 4, 2009, 3–14.
- [5] Sha W., Malinov S., *Titanium Alloys Modelling of Microstructure. Properties and Applications*, Woodhead Publishing, Cornwall 2009.
- [6] Słodki B., Zębala W., Struzikiewicz G., *Correlation between cutting data selection and chip form in stainless steel turning*, Machining Science and Technology 19/2, 2015, 217–235.



- [7] Ślusarczyk Ł., Franczyk E., *Development and verification of a measuring stand for recording the physical phenomena during turning*, Photonics Applications in Astronomy Communications Industry and High-Energy Physics Experiments Book Series, Proceedings of SPIE 10445, 104456G, 2017.
- [8] Ślusarczyk Ł., *The construction of the milling process simulation models*, Photonics Applications in Astronomy Communications Industry and High-Energy Physics Experiments Book Series: Proceedings of SPIE 10031, 100310C, 2016.
- [9] Ślusarczyk Ł., Franczyk E., *Experimental determination of forces in a cutting zone during turning a stainless steel shaft*, Czasopismo Techniczne 5-M/2011.
- [10] Yang W.H., Tarng, Y.S., *Design optimization of cutting parameters for turning operations based on the Taguchi method*, J. Mater. Process. Technol. 84, 1998, 122–129.